



ELSEVIER

27 May 2002

Physics Letters A 298 (2002) 18–28

PHYSICS LETTERS A

www.elsevier.com/locate/pla

Stability and optimization of chaos synchronization through feedback coupling with delay

Y. Chembo Kouomou^{a,b}, P. Woafu^{a,*}

^a *Laboratoire de Mécanique, Faculté des Sciences, Université de Yaoundé I, B.P. 812, Yaoundé, Cameroon*

^b *Ecole Nationale Supérieure des Postes et Télécommunications, Yaoundé, Cameroon*

Received 10 July 2001; received in revised form 12 October 2001; accepted 12 December 2001

Communicated by A.P. Fordy

Abstract

We perform the stability and optimization analysis for the (non)delayed synchronization of Duffing-like oscillators, using a retroactive scheme. Stability boundaries are derived through Floquet theory. Critical values for the feedback synchronization coefficient are found. The influence of the delay and of the onset time of the driving upon stability and synchronization time is also analyzed. © 2002 Elsevier Science B.V. All rights reserved.

1. Introduction

The very essence of chaos is complexity, unpredictability and extreme sensitivity to initial conditions. It is therefore counterintuitive to suppose that chaotic oscillators can synchronize, i.e., continuously remain in step with each other. Nevertheless, when certain requirements are met, it is possible to obtain a high correlation between several identical or different chaotic systems [1–6]. During recent years, different schemes have been developed for this purpose to be achieved. Generally, in the synchronization's mechanism, a “master” system drives or commands the response of a “slave” system, even though other techniques with mutual coupling, which ignore this hierarchy, have been set up.

Very soon, it appeared that one of the most important application of chaotic synchronization is the masking of information-bearing signals in spread-spectrum communications [7–9], although researchers still explore applications in the areas of oscillatory neural systems, multimode laser systems or chemical processes.

In this Letter, we aim to study the stability and the optimization of (non)delayed synchronization. In fact, deep stability analysis is scarcely performed in literature as far as synchronization is concerned, despite its crucial importance. On the other hand, optimization is a key-word for wide-spread applications, and efforts should be made to fulfill optimization criteria such as the minimization of both synchronization time and required energy input for the process. Delayed synchronization also gathers a growing interest, since it enables the modelization in wireless telecommunications, coupled phase-locked loops systems or neuronal networks.

* Corresponding author.

E-mail address: pwoafu@uycdc.uninet.cm (P. Woafu).

For the illustration of our approach, we will take a very well known model of nonlinear physics, the single-well Duffing oscillator, with either a positive or a negative nonlinear stiffness term. We also choose to achieve the synchronization through a feedback coupling, so that the whole system becomes

$$\begin{cases} \ddot{x} + \lambda\dot{x} + x + \gamma x^3 = F \cos \omega t, \\ \ddot{u} + \lambda\dot{u} + u + \gamma u^3 \\ = F \cos \omega t - K(u - x_\tau)H(t - T_0), \end{cases} \quad (1)$$

where H is the Heaviside function defined as

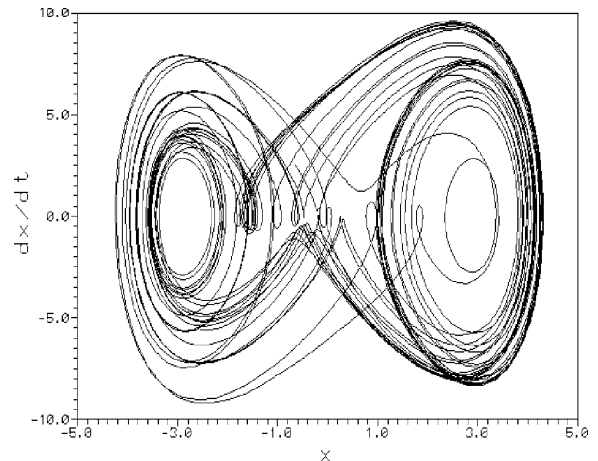
$$H(x) = \begin{cases} 0 & \text{if } x < 0, \\ 1 & \text{if } x \geq 0, \end{cases} \quad (2)$$

t is the time, and T_0 is the onset time of the synchronization. x represents the master system, and u the slave system. τ is the delay, assuming that $x_\tau(t) = x(t - \tau)$. Hence the role of the feedback coupling coefficient K will be to force the convergence of u towards the given past state x_τ of the master oscillator x . It has been proven that this synchronization scheme efficiently resists to noise, and can easily be implemented practically [4].

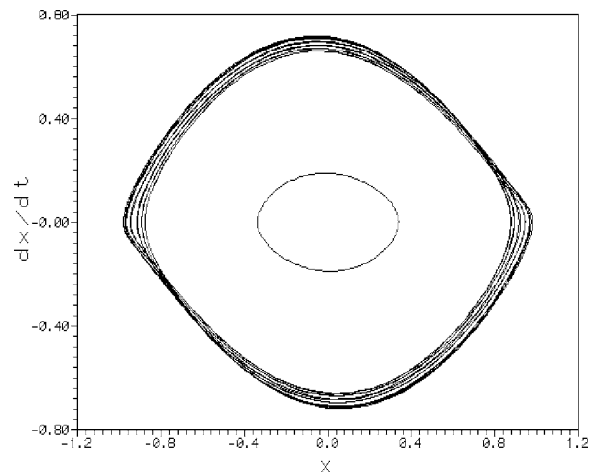
The Letter is organized as follows. In Section 2, we perform the stability analysis of the synchronization when $\tau = 0$. Floquet theory will enable to derive approximations for the stability boundaries, and qualitatively explain their occurrence. In Section 3, the delay τ is taken into account. Its influence upon stability is studied, and we also analytically derive the critical value K_{cr} under which, for a given precision, no synchronization is possible. Section 4 deals with the duration of synchronization, as well as its variations as a function of K and T_0 . We finally conclude in Section 5. The numerical simulation of all ordinary differential equations will use the fourth-order Runge–Kutta algorithm, with a time step $h_{RK} = T/500$, where $T = 2\pi/\omega$ is the period of the external excitation.

2. Stability and synchronization of the coupled chaotic system ($\tau = 0$)

According to the chosen parameters, the single-well Duffing model can display a chaotic dynamics. In the $\gamma > 0$ case [10,11], high external excitation gives rise to chaotic oscillations owing to a pseudo-two-wells potential configuration, as it appears in Fig. 1(a).



(a)



(b)

Fig. 1. Phase plane of the chaotic oscillators. (a) $\gamma > 0$ case: $\lambda = 0.2$, $\gamma = 1.0$, $F = 28.5$, $\omega = 0.86$, with initial conditions $(0, 0)$. (b) $\gamma < 0$ case: $\lambda = 0.4$, $\gamma = -1.0$, $F = 0.23$, $\omega = 0.5255$, with initial conditions $(0, 0)$ for the inner limit cycle and $(-0.3, 0.7)$ for the chaotic trajectory.

Chaos is much more difficult to spot when $\gamma < 0$ [12]. For example, we have in Fig. 1(b) a set of parameters which induces two different stable orbits according to initial conditions, i.e., an inner regular limit cycle and an outer chaotic trajectory. Note that throughout all the Letter, the $\gamma > 0$ and $\gamma < 0$ cases will always refer to the sets of parameters used, respectively, in Figs. 1(a) and (b).

Starting from T_0 , the coupling becomes effective and the system changes its configuration: hence stabil-

ity considerations come into play. We emphasize that stability is obviously not synchronization, because the notion of synchronization implies the negativity of the sub-Lyapunov exponents, while stability, which is less restrictive, just requires u to remain bounded. Therefore, one can tolerate the synchronization to fail, but never to be unstable since it would cause irreversible damages to the system.

Let us introduce a new variable

$$\varepsilon(t) = u(t) - x(t), \quad (3)$$

which is the measure of the relative nearness of both chaotic orbits. The stability of the synchronization process is therefore strictly equivalent to the boundedness of ε , which obeys to

$$\ddot{\varepsilon} + \lambda \dot{\varepsilon} + (1 + K + 3\gamma x^2)\varepsilon + 3\gamma x \varepsilon^2 + \gamma \varepsilon^3 = 0. \quad (4)$$

Eq. (4), which is nonlinear with a parametric excitation, can lead to unbounded solutions according to the coefficient K . Since the parametric excitation is also chaotic, the analytic approach of the stability study is quite difficult. We are therefore compelled to use approximations for both $\gamma > 0$ and $\gamma < 0$ cases.

In occurrence, we will replace the chaotic trajectories by virtual regular elliptic trajectories of the form

$$\bar{x} = \bar{x}_0 \cos(\omega t - \varphi), \quad (5)$$

where \bar{x} obeys to the variational Ritz criterion

$$\int_0^{2\pi/\omega} [F \cos \omega t - (\ddot{\bar{x}} + \lambda \dot{\bar{x}} + \bar{x} + \gamma \bar{x}^3)] e^{i\omega t} dt = 0. \quad (6)$$

Eq. (6) yields the following set of nonlinear algebraic equations:

$$\left[\left((1 - \omega^2) + \frac{3}{4} \gamma \bar{x}_0^2 \right)^2 + (\lambda \omega)^2 \right] \bar{x}_0^2 = F^2, \quad (7)$$

$$\varphi = \tan^{-1} \left[\frac{\lambda \omega}{(1 - \omega^2) + \frac{3}{4} \gamma \bar{x}_0^2} \right].$$

One can hence find that the corresponding solution for the $\gamma > 0$ case is

$$\bar{x}_0 = 3.32372 \quad \text{and} \quad \varphi = 0.02008, \quad (8a)$$

and for the $\gamma < 0$ case,

$$\bar{x}_0 = 0.86479 \quad \text{and} \quad \varphi = 0.91134. \quad (8b)$$

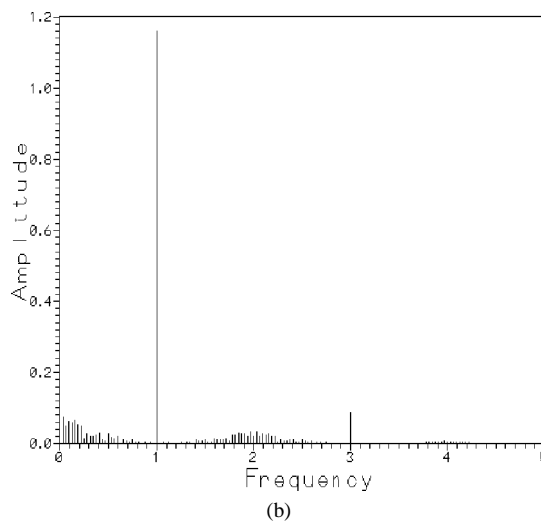
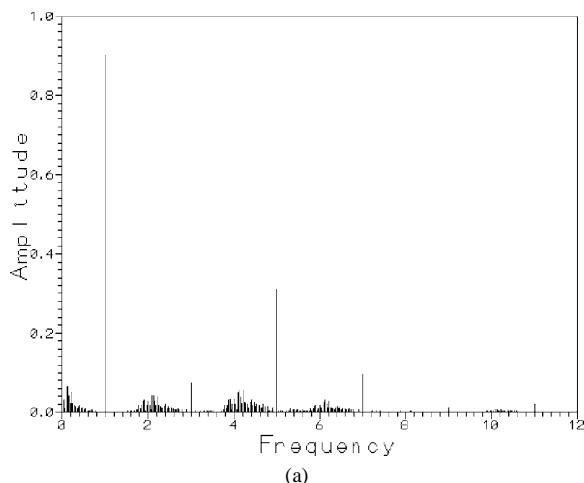


Fig. 2. Fourier spectra, with frequencies in units of ω and amplitudes in units of related \bar{x}_0 . (a) $\gamma > 0$ case. (b) $\gamma < 0$ case.

Fig. 2(a) displays the Fourier spectrum of the $\gamma > 0$ Duffing oscillator. Energy is mainly distributed in very sharp bands around odd harmonics of ω . Hence, Ritz approximation is qualitatively poor (this could have been predicted earlier from the phase plane in Fig. 1(a)), but nevertheless remains of quantitative interest since the major part of the energy lays around the fundamental frequency ω . On the other hand, for the $\gamma < 0$ case, the phase plane (Fig. 1(b)) and the Fourier spectrum (Fig. 2(b)) both agree that the Ritz approximation is rather good, so that it can be used to perform the stability analysis.

Therefore, if we only keep the linear terms in ε (since ε is assumed to be small), the stability of the synchronization would be established by the study of the linear parametric equation

$$\ddot{\varepsilon} + \lambda \dot{\varepsilon} + [\Omega_0^2 + \mu \cos(2\omega t - 2\varphi)]\varepsilon = 0, \quad (9)$$

where

$$\begin{aligned} \Omega_0^2 &= 1 + K + \frac{3}{2}\gamma\bar{x}_0^2, \\ \mu &= \frac{3}{2}\gamma\bar{x}_0^2, \end{aligned} \quad (10)$$

\bar{x}_0 and φ being the coefficients of the Ritz solutions. Eq. (9) is a damped version of the Mathieu equation, and presents instability domains according to λ , Ω_0 , ω and μ . Floquet theory tackles this problem by pre-cising the stability boundaries. Setting the following rescalings:

$$\begin{aligned} z &= \omega t, \\ \eta(z) &= \varepsilon \exp\left(\frac{\lambda z}{2\omega}\right), \end{aligned} \quad (11)$$

the dissipative Mathieu equation can be written in the canonical form as

$$\ddot{\eta} + [\delta + 2\alpha \cos(2z - 2\varphi)]\eta = 0 \quad (12)$$

with

$$\begin{aligned} \delta &= \frac{1}{\omega^2} \left[\Omega_0^2 - \frac{\lambda^2}{4} \right] = \frac{1}{\omega^2} \left[1 + K + \frac{3}{2}\gamma\bar{x}_0^2 - \frac{\lambda^2}{4} \right], \\ \alpha &= \frac{\mu}{2\omega^2} = \frac{3\gamma\bar{x}_0^2}{4\omega^2}. \end{aligned} \quad (13)$$

The feedback parameter K only modifies δ , but not α anyway. The solution of Eq. (12) has the form

$$\eta(z) = e^{\theta z} \phi(z), \quad (14)$$

where θ is a complex number, and

$$\phi(z) = \sum_{n=-\infty}^{+\infty} \phi_n e^{2inz} \quad (15)$$

is a π -periodic function. Hence,

$$\eta(z) = \sum_{n=-\infty}^{+\infty} \phi_n e^{(\theta+2in)z}. \quad (16)$$

Inserting Eq. (16) in Eq. (12) gives an infinite homogeneous linear algebraic system, which may have

solutions if and only if the associated determinant is set equal to zero, that is,

$$\begin{aligned} \Delta(\theta) &= \left\| \frac{(\delta + (\theta + 2in)^2)\delta_{m,n}}{\delta - (2n)^2} \right. \\ &\quad \left. + \frac{\alpha(e^{2i\varphi}\delta_{m-1,n} + e^{-2i\varphi}\delta_{m+1,n})}{\delta - (2n)^2} \right\| \\ &= 0, \end{aligned} \quad (17)$$

where the $\delta_{m,n}$ are Kronecker symbols [13]. $\Delta(\theta)$ is called the infinite Hill determinant, and one can show that

$$\Delta(\theta) = \Delta(0) - \frac{\sin^2\left(\frac{1}{2}i\pi\theta\right)}{\sin^2\left(\frac{1}{2}\pi\sqrt{\delta}\right)}. \quad (18)$$

Therefore

$$\theta = \pm \frac{2i}{\pi} \sin^{-1} \sqrt{\Delta(0) \sin^2\left(\frac{1}{2}\pi\sqrt{\delta}\right)}. \quad (19)$$

Since, from Eqs. (11),

$$\varepsilon(z) = \phi(z) \exp\left[\left(\theta - \frac{\lambda}{2\omega}\right)z\right], \quad (20)$$

ε oscillations either decay to zero or increase to infinity, unless $\text{Re}(\theta) = \lambda/2\omega$. According to Floquet theory, the transition from stability to instability (or the inverse) occurs only in two conditions:

- π -periodic transition: $\theta = \lambda/2\omega$,

$$\Delta(0) + \frac{\sinh^2\left(\frac{\lambda\pi}{4\omega}\right)}{\sin^2\left(\frac{1}{2}\pi\sqrt{\delta}\right)} = 0. \quad (21)$$

- 2π -periodic transition: $\theta = i + \lambda/2\omega$,

$$\Delta(0) - \frac{\cosh^2\left(\frac{\lambda\pi}{4\omega}\right)}{\sin^2\left(\frac{1}{2}\pi\sqrt{\delta}\right)} = 0. \quad (22)$$

If we define the new real function

$$\Gamma(\delta, \alpha) = \begin{cases} \Delta(0) \sin^2\left(\frac{1}{2}\pi\sqrt{\delta}\right) & \text{if } \delta \geq 0, \\ -\Delta(0) \sinh^2\left(\frac{1}{2}\pi\sqrt{-\delta}\right) & \text{if } \delta < 0, \end{cases} \quad (23)$$

the analytic stability condition is the following, according to Hopf theorem:

$$-\sinh^2\left(\frac{\lambda\pi}{4\omega}\right) < \Gamma(\delta, \alpha) < +\cosh^2\left(\frac{\lambda\pi}{4\omega}\right). \quad (24)$$

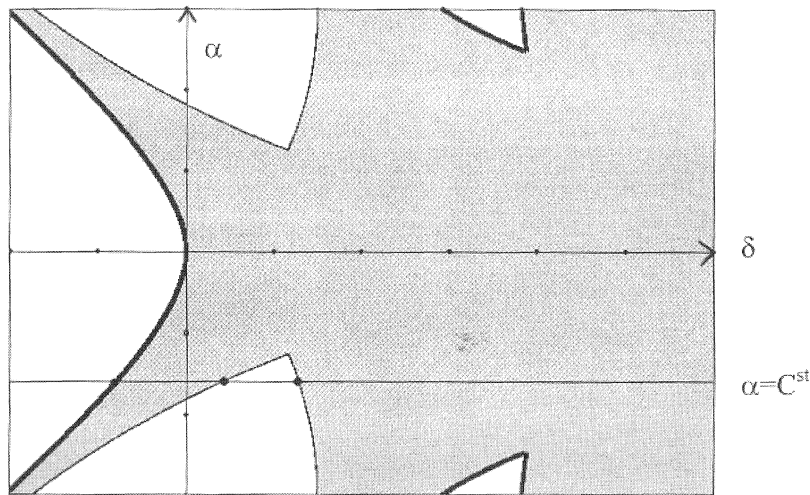


Fig. 3. Stability diagram in the (δ, α) plane showing the π -periodic boundaries (thick lines) and 2π -periodic boundaries (thin lines).

Graphically, Eqs. (21) and (22) define a set of curves in the (δ, α) plane, as approximately represented in Fig. 3 (for exact figures see Refs. [13–15]). For a fixed α , the Hopf theorem demonstrates that the stable values of δ are those which are strictly situated between boundaries of different types: the stability domain is hence the shaded area of Fig. 3. Because α is independent of K , the figurative point of the system in the (δ, α) plane is just moving along a $\alpha = \text{const}$ straight horizontal line when K is varied. Starting from $\delta = -\infty$ (i.e., $K = -\infty$ according to Eqs. (13)), this point will alternatively pass through unstable and stable domains.

We should not forget that the Ritz orbit is only an approximation of the chaotic trajectory. In the best case ($\gamma < 0$), we can consider that the Ritz solution is correct with an uncertainty $(\delta\bar{x}_0)$ for the amplitude \bar{x}_0 . Hence, from stability boundaries (24), the width $(\delta\Gamma)$ of the inner safety intervals will be

$$(\delta\Gamma) = \begin{cases} \left| \left(\frac{\partial\Delta(0)}{\partial\bar{x}_0} \sin^2\left(\frac{1}{2}\pi\sqrt{\delta}\right) + \frac{3\pi\gamma\bar{x}_0}{4\omega^2} \frac{\sin(\pi\sqrt{\delta})}{\sqrt{\delta}} \Delta(0) \right) (\delta\bar{x}_0) \right| & \text{if } \delta \geq 0, \\ \left| \left(-\frac{\partial\Delta(0)}{\partial\bar{x}_0} \sinh^2\left(\frac{1}{2}\pi\sqrt{-\delta}\right) + \frac{3\pi\gamma\bar{x}_0}{4\omega^2} \frac{\sinh(\pi\sqrt{-\delta})}{\sqrt{-\delta}} \Delta(0) \right) (\delta\bar{x}_0) \right| & \text{if } \delta < 0. \end{cases} \quad (25)$$

The accuracy of these boundaries will obviously depend on the order of truncation of the infinite deter-

minant $\Delta(0)$. The agreement between numerical simulations and the analytic approach is qualitatively effective. For the $\gamma > 0$ case, we have a single stability boundary value $K_{b1} \approx -6.0$ above which the coupled system is stable. A deeper investigation involving at least the odd harmonics of ω in the approximation of x would be able to explain why, despite the high α value, only a single boundary value is found. The $\gamma < 0$ case fits better to the analytic study, since here the lower $|\alpha|$ induces two stability intervals of the kind $]K_{b1}, K_{b2}[$ and $]K_{b3}, +\infty[$. These intervals correspond to the two segments laying in the shaded area of Fig. 3, and the boundary values are numerically found to be $K_{b1} = -0.000$, $K_{b2} = 0.088$ and $K_{b3} = 1.312$. Obviously, $K = 0$ which corresponds to an uncoupled system always belongs to a stability interval.

It has been demonstrated that synchronization occurs when negative sub-Lyapunov exponents are obtained [1]. In fact, the above stability analysis enables to derive that for the $\gamma < 0$ case, the related sub-Lyapunov exponent can be approximated by

$$\Lambda \approx \text{Re} \left(\theta - \frac{\lambda}{2\omega} \right), \quad (26)$$

so that stability areas should be strictly identified to synchronization areas. Numerical simulations confirm this hypothesis, and effectively, the slave oscillator u either synchronizes with x (in the whole stability zone) or either becomes unstable. This is absolutely not the case for the $\gamma > 0$ system, since in that case one can

found stable intervals without effective synchronization. Indeed, in this latter case, the approximate virtual orbit is very poor and instantaneous deviations (bursts) from this virtual orbit are frequent and certainly have high amplitudes. Consequently, high quality results cannot be attained [16–18].

3. Delayed synchronization ($\tau \neq 0$)

The purpose of delayed feedback synchronization is to achieve the convergence of $u(t)$ towards $x(t - \tau) = x_\tau(t)$, i.e., to ensure a constant phase shift between both chaotic oscillators. Applications for this scheme recently appeared to be wide, particularly for wireless synchronization devices. An extension of this topic can lead to the synchronization of distributed delayed systems, with application to private communications [19]. In some particular cases, one can even couple the driven systems in such a way that they anticipate the driver by synchronizing with its arbitrarily distant future state. This anticipated synchronization scheme would probably enable fast prediction in electronic or optical devices in communication systems [20].

When delay is taken into account, ε rather obeys to

$$\ddot{\varepsilon} + \lambda \dot{\varepsilon} + (1 + K + 3\gamma x_\tau^2)\varepsilon + 3\gamma x_\tau \varepsilon^2 + \gamma \varepsilon^3 = -2F \sin \frac{\omega\tau}{2} \sin \left(\omega t - \frac{\omega\tau}{2} \right). \quad (27)$$

ε is now submitted to an external sinusoidal excitation whose amplitude depends on F and τ . From this point, quite important remarks have to be made. When τ is a multiple of the period $T = 2\pi/\omega$ (i.e., $\tau = nT$, n being a positive integer), this external term vanishes and Eq. (27) is no more different from Eq. (4). Hence, when $\tau = nT$, the whole analysis developed in Section 2 remains valid. On the other hand, when $\tau \neq nT$, the external excitation (due to F and τ) induces steady state oscillations for ε , and then fights against the uniform collapsing between u and x_τ . Stability is hence highly affected by these oscillations, mostly when ε is strongly excited. In fact, the most unfavorable scheme occurs when τ is an odd multiple of $T/2$.

When $\tau = nT$, instability mainly comes from the parametric excitation, as we have earlier seen. But

when $\tau \neq nT$, amplitudes of ε can be very large depending on F and τ , and therefore, nonlinearity may no longer be discarded as we did for Eq. (9): it rather implies crucial modifications.

Let us take the example of the $\gamma < 0$ case. If we suppose

$$\varepsilon = E \cos(\omega t - \psi), \quad (28)$$

the amplitude E according to Eq. (27) approximately obeys to a twelfth-order polynomial equation (explicitly defined in Appendix A) of the form

$$\sum_{k=0}^6 m_k (E^2)^k = 0. \quad (29)$$

It is well known that the (E, K) curve in this case leads to multivalued areas, which correspond to the hysteresis phenomenon. This means that, according to K , the stability of the system can also depend on the initial conditions $(\varepsilon(T_0), \dot{\varepsilon}(T_0))$. Since, precisely, $\varepsilon(T_0) = u(T_0) - x(T_0)$ is unpredictable and exclusively depends on T_0 , one can reach the surprising conclusion that there exist intervals of K where the onset time of the driving T_0 randomly decides the stability of the synchronization process. Numerical simulation confirms this analysis. For example, if we suppose $\tau = T/2$ in the $\gamma < 0$ case, we notice that synchronization is unstable when $T_0 = 105$ while it remains stable when $T_0 = 102$ (initial conditions being specified in Fig. 4).

Therefore, if $\tau \neq nT$, K must be chosen with very much care. We first have to avoid “standard” instability intervals (induced by the linear parametric excitation), but also the above “ambiguous” ones (induced by nonlinearity). Unfortunately, these latter areas cannot be determined analytically. Nevertheless, a summary analysis would advice to always avoid the neighborhood of K values which induce parametric or nonlinear resonance. These risky resonance frequencies can be analytically checked, for example, through the multiple time scales method.

The second incidence of the delay τ on the stability of the system lies on the standard parametric stability intervals. In fact, if Eq. (27) was linear, the external excitation term of ε would have absolutely not induced any modification to the stability analysis of Section 2. But in our case, nonlinearity qualitatively modifies

the stability pattern. For example, in the $\gamma < 0$ case, numerical simulations have shown that the second (and compact) instability interval rapidly disappears when τ is far from nT .

As far as synchronization is concerned, suitable values of K must obviously fulfill all the above stability conditions, but also the more restrictive synchronization requirements. Rigorously, we are allowed to speak about synchronization exclusively when $\tau = nT$. It is only under this condition that sub-Lyapunov exponents can decide the occurrence of synchronization. When $\tau \neq nT$, it would be more appropriate to speak about the control of a chaotic trajectory towards another chaotic trajectory, because in this case, the variational variables never exponentially decay to zero. Nevertheless, since there are exclusively chaotic oscillators into play, we will continue to speak about synchronization independently of the value of τ , and our synchronization condition will rather be

$$|\varepsilon(t)| < h, \quad t > (T_0 + T_{\text{syn}}), \quad (30)$$

where h is the precision of the synchronization, and T_{syn} its duration, that is, the interval of time between the onset time of the driving and the time of its end. The stability analysis suggests that very large K values are always good, but it would be very interesting to determine the critical value K_{cr} under which, for a given precision, synchronization is impossible. The aim of such an investigation is at least twofold: it first enables to achieve the process with the lowest K possible, which corresponds to the lowest energy inputs; secondly, it permits to know how the parameters of the system affect this critical value.

Small amplitudes for ε are obtained when Ω_0 is far beyond ω . Under this latter condition, we are allowed to neglect nonlinearities ($\varepsilon \ll 1$) and to discard the linear parametric excitation ($\Omega_0 \gg \mu$) and therefore, ε approximately obeys to the following linear differential equation:

$$\ddot{\varepsilon} + \lambda \dot{\varepsilon} + \Omega_0^2 \varepsilon = -2F \sin \frac{\omega\tau}{2} \sin \left(\omega t - \frac{\omega\tau}{2} \right). \quad (31)$$

After the main resonance peak, the amplitude of the steady state oscillations of ε is a decreasing function of Ω_0 (i.e., of K). The critical value K_{cr} is precisely found by setting the equality between this amplitude

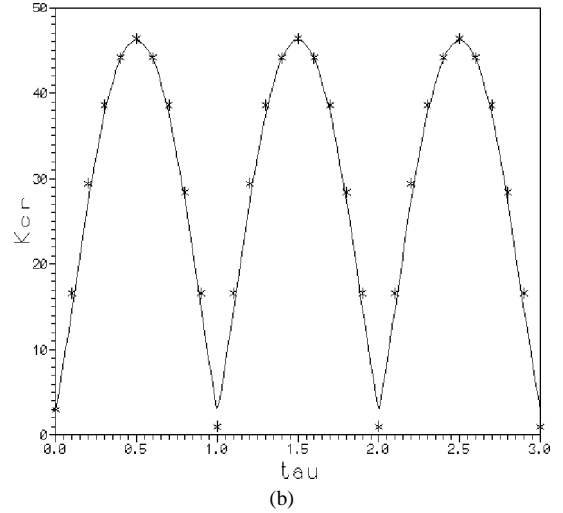
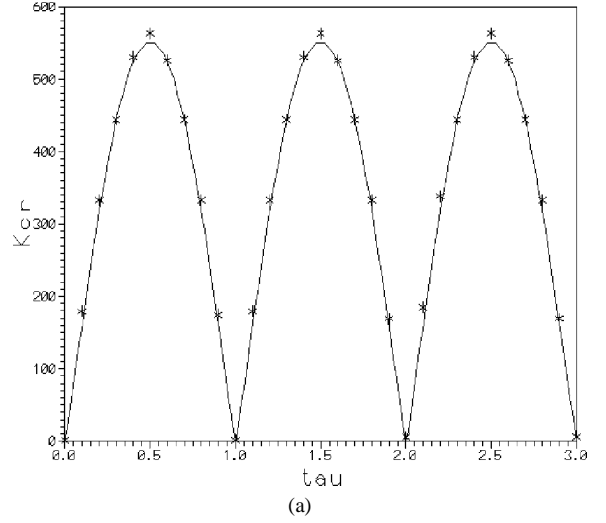


Fig. 4. K_{cr} as a function of τ (full lines for analytic results, stars for numerical results). τ is in units of T . (a) $\gamma > 0$ case. $h = 10^{-1}$. Initial conditions for the x and u oscillators are, respectively, $(0, 0)$ and $(1, 0)$. (b) $\gamma < 0$ case. $h = 10^{-2}$. Initial conditions for the x and u oscillators are, respectively, $(-0.3, 0.7)$ and $(-0.6, 0.6)$.

and the precision h , so that

$$K_{\text{cr}} = \omega^2 - 1 - \frac{3}{2} \gamma \bar{x}_0^2 + \sqrt{\left(\frac{2F}{h} \sin \frac{\omega\tau}{2} \right)^2 - (\lambda\omega)^2}. \quad (32)$$

Figs. 4 and 5 show the excellent concordance between formula (32) and the results of the numerical simulation of the differential system (1). It appears that K_{cr} is a decreasing function of h , and a periodic

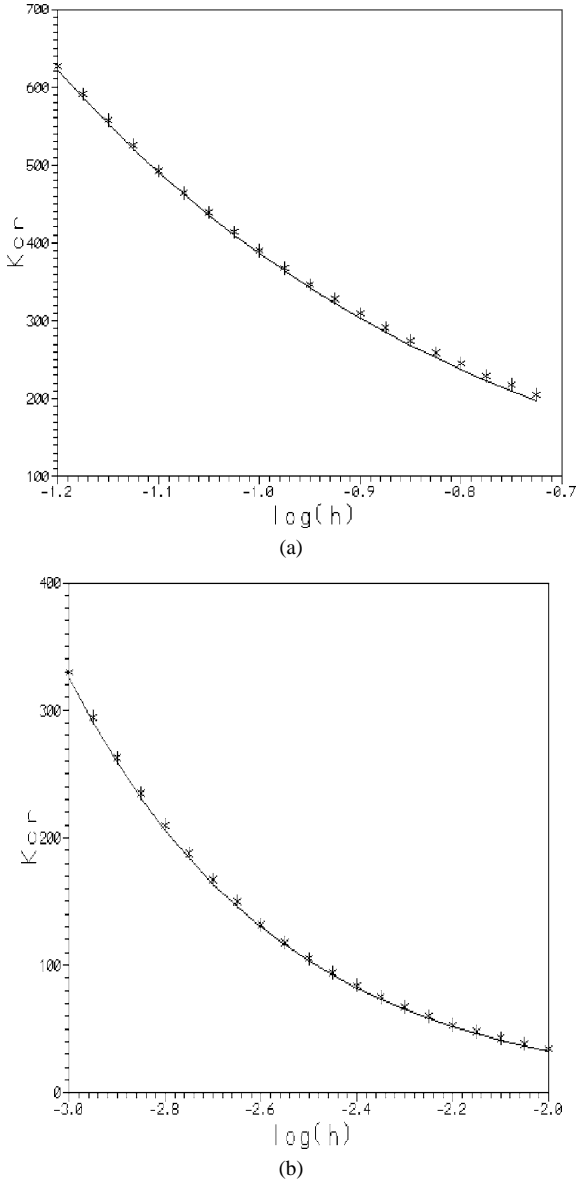


Fig. 5. K_{cr} as a function of $\log_{10}(h)$ (full lines for analytic results, stars for numerical results). (a) $\gamma > 0$ case. $\tau = T/4$. Initial conditions for the x and u oscillators are as in Fig. 4. (b) $\gamma < 0$ case. $\tau = T/4$. Initial conditions for the x and u oscillators are as in Fig. 4.

function of τ . It is quite noticing that large values of K are necessary to ensure the synchronization when $\tau \neq nT$, even for a very poor precision. In these cases, great energy inputs are required, mainly when $\tau = (2n + 1)T/2$.

It should not be forgotten that the validity of formula (32) is limited by the condition

$$\left| \sin \frac{\omega\tau}{2} \right| > \frac{\lambda\omega h}{2F}, \quad (33)$$

and then does not apply when $\tau = nT$. In these cases, very low values are observed ($K_{cr} \sim 1$) for very high precision ($h \sim 10^{-5}$). In fact, the proper analysis would rather here correspond to the computation of the θ exponent as a function of K . Anyway, these τ values fit with the most favorable situations in both dynamic (excellent precision) and energetic (low K) points of view.

4. Duration of synchronization

The synchronization process can be considered as optimized when a low energy input succeeds in ensuring a fast synchronization. This latter aspect should absolutely not be marginalized. If we consider, for example, the application of synchronization in secure communications, the range of time T_{syn} during which the chaotic oscillators are not synchronized corresponds to the range of time during which the encoded message can unfortunately not be recovered. More than a grave and irreversible lost of information, this is a catastrophe in digital telecommunications, since the first bits of standardized bit strings always contain signalization data, i.e., the “identity card” of the message. Hence, it clearly appears that T_{syn} has to be minimized, so that the chaotic oscillators synchronize as fast as possible.

In our system, T_{syn} corresponds to the transient oscillations, which can be supposed as completely decayed when they are still below h , even when added to steady-state oscillations. From Eq. (31), we can therefore obtain

$$T_{syn} = \frac{2}{\lambda} \ln \left[\frac{\sqrt{\varepsilon^2(T_0) + \frac{(\dot{\varepsilon}(T_0) + \lambda\varepsilon(T_0)/2)^2}{\Omega_0^2 - \lambda^2/4}}}{h - \frac{|2F \sin(\omega\tau/2)|}{\sqrt{(\Omega_0^2 - \omega^2)^2 + (\lambda\omega)^2}}} \right]. \quad (34a)$$

One can notice that T_{syn} increases logarithmically with the initial separation between chaotic orbits in the phase plane, but decreases with K towards a minimum value which is

$$T_{syn \min} = \lim_{K \rightarrow +\infty} T_{syn} = \frac{2}{\lambda} \ln \left[\frac{|\varepsilon(T_0)|}{h} \right]. \quad (34b)$$

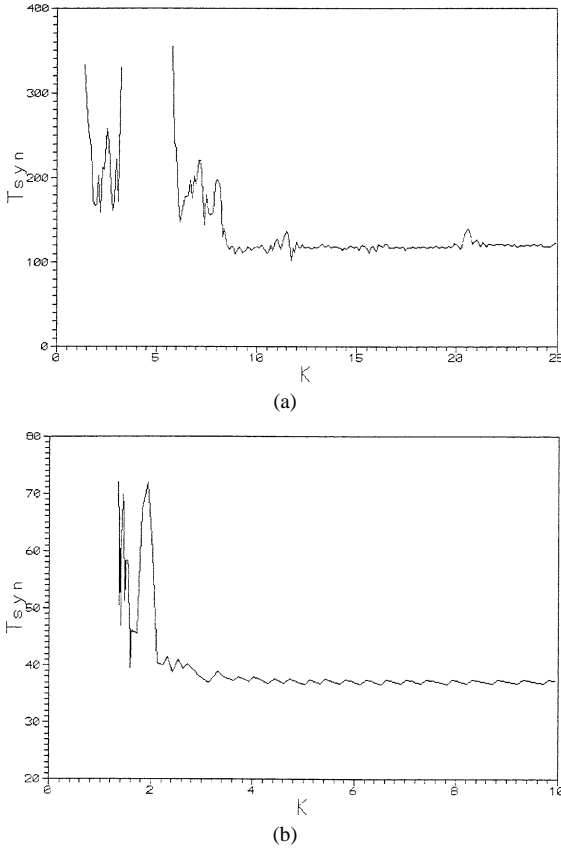


Fig. 6. T_{syn} as a function of K when $\tau = 0$ (numerical results). (a) $\gamma > 0$ case. $T_0 = 100$ and $h = 10^{-5}$. Initial conditions for the x and u oscillators are as in Fig. 4. (b) $\gamma < 0$ case. $T_0 = 100$ and $h = 10^{-5}$. Initial conditions for the x and u oscillators are as in Fig. 4.

Hence, our analysis points out a minimal asymptotic duration under which no synchronization occurs. This is of great practical interest, since one could have naively thought that the synchronization could have been led as fast as desired, just depending on K . Therefore, we are hereby prevented from a useless increase of K , i.e., from an unavailing waste of input energy. Figs. 6 and 7 confirm that very large K values are not necessary to ensure the synchronization with approximately the minimum T_{syn} .

Formula (34) does not explain the serrated structure of the curves in Figs. 6 and 7 obtained through the numerical simulation of Eqs. (1). In fact, this phenomenon can be explained by the Floquet theory. We have earlier introduced the θ exponent, whose real part

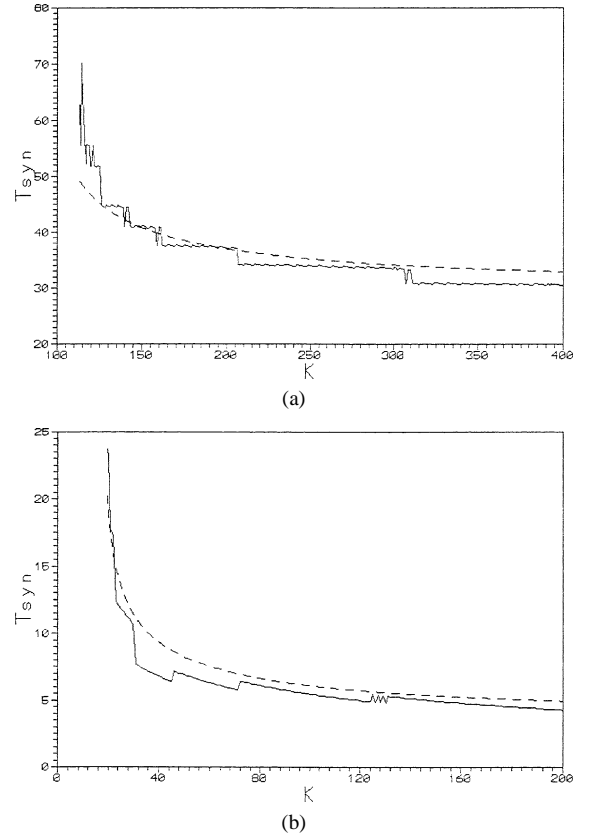


Fig. 7. T_{syn} as a function of K when $\tau \neq 0$ (dashed lines for analytic results, full lines for numerical results). (a) $\gamma > 0$ case. $T_0 = 100$, $h = 10^{-1}$ and $\tau = T/16$. Initial conditions for the x and u oscillators are as in Fig. 4. (b) $\gamma < 0$ case. $T_0 = 100$, $h = 10^{-2}$ and $\tau = T/8$. Initial conditions for the x and u oscillators are as in Fig. 4.

permits to determine the decay rate of the parametric oscillations. It can be explicitly defined as follows:

$$\begin{aligned}
 & -\sinh^2\left(\frac{\lambda\pi}{4\omega}\right) < \Gamma < 0: \\
 & \theta = \pm 2i \pm \frac{2}{\pi} \sinh^{-1} \sqrt{-\Gamma}, \\
 & 0 \leq \Gamma \leq 1: \\
 & \theta = \pm \frac{2i}{\pi} \sin^{-1} \sqrt{\Gamma}, \\
 & 1 < \Gamma < +\cosh^2\left(\frac{\lambda\pi}{4\omega}\right): \\
 & \theta = \pm i \pm \frac{2}{\pi} \cosh^{-1} \sqrt{\Gamma}.
 \end{aligned} \tag{35}$$

One can therefore derive the associated durations of synchronization

$$-\sinh^2\left(\frac{\lambda\pi}{4\omega}\right) < \Gamma < 0:$$

$$\tilde{T}_{\text{syn}} = T_{\text{syn}} \frac{1}{1 - \frac{4\omega}{\lambda\pi} \sinh^{-1} \sqrt{-\Gamma}},$$

$$0 \leq \Gamma \leq 1:$$

$$\tilde{T}_{\text{syn}} = T_{\text{syn}},$$

$$1 < \Gamma < +\cosh^2\left(\frac{\lambda\pi}{4\omega}\right):$$

$$\tilde{T}_{\text{syn}} = T_{\text{syn}} \frac{1}{1 - \frac{4\omega}{\lambda\pi} \cosh^{-1} \sqrt{+\Gamma}}, \quad (36)$$

where \tilde{T}_{syn} is the new duration of synchronization, and T_{syn} the former one defined by Eqs. (34). An increase of K leads to a variation of $\Gamma(\delta, \alpha)$, and then induces a modulation of T_{syn} mainly when $\Gamma(\delta, \alpha)$ is not between 0 and 1.

Further investigations can even allow to foresee the occurrence of these sharp local maxima observed in Figs. 6 and 7. From Floquet theory, we know that at the first approximation, linear parametric resonance arises when

$$\delta = n^2, \quad (37)$$

n being a positive integer. The corresponding K values are

$$K_n = n^2\omega^2 - \left(1 + \frac{3}{2}\gamma\bar{x}_0^2 - \frac{\lambda^2}{4}\right) \quad (38)$$

according to Eqs. (13). It is possible to ameliorate the accuracy of the above statements by a better analytic approach of the chaotic oscillations, and also by considering higher- and lower-order nonlinear and parametric resonance.

5. Conclusion

In this Letter, we have led a stability and optimization analysis of the continuous feedback synchronization process. Floquet theory has enabled us to explain the occurrence of stability intervals, as well as the irregular structure of the K - T_{syn} curve. The influence of the delay has also been investigated. It has been found

that the minimal feedback coefficient K_{cr} which enables the synchronization is a periodic function of τ . We have also demonstrated that when K increases, an asymptotic minimal value of T_{syn} is reached.

It would be very interesting to extend the study to other models of synchronization. For example, the Boccaletti et al. adaptive synchronization scheme [5] and the original Pecora and Carroll method [1] can be mathematically assimilated to some modified versions of the retroactive method we have considered, the modification being, respectively, a periodically updated K and an infinite K . Hence, if we accordingly modify all the analysis we have developed in this Letter, interesting conclusions may be drawn for these neighboring cases. One can even investigate how feeding back more variables (through a feedback gain matrix) can ameliorate the synchronization conditions. A link has also to be made for the synchronization of multidimensional and hyperchaotic systems, in view of practical applications. We are confident that a more realistic modelization of chaotic oscillations taking into account stochasticity would probably strengthen the comprehension of the whole synchronization process, despite its complexity.

Appendix A

For the resolution of Eq. (27), we use the harmonic balance method. The chaotic variable x_τ is replaced by the related virtual Ritz orbit, and the randomness of phase shifts allows us to discard them in first approximation. Exception has been made for ψ , for which we have set $\langle \cos^2 \psi \rangle = 1/2$. Therefore, if

$$\begin{aligned} \mathcal{E}_c = & -\frac{3}{2}\gamma\bar{x}_0E^2 \left[E(\Omega_0^2 - \omega^2) - \frac{3}{4}\gamma\bar{x}_0^2E + \frac{3}{4}\gamma E^3 \right] \\ & + \left[2\lambda E\omega F \sin \frac{\omega\tau}{2} \right], \end{aligned}$$

$$\begin{aligned} \mathcal{E}_s = & -2F \sin \frac{\omega\tau}{2} \left[E(\Omega_0^2 - \omega^2) + \frac{3}{4}\gamma\bar{x}_0^2E + \frac{3}{4}\gamma E^3 \right] \\ & - \frac{3}{2}\gamma\bar{x}_0E^2[\lambda E\omega], \end{aligned}$$

$$\begin{aligned} \mathcal{E}_0 = & \left[E(\Omega_0^2 - \omega^2) + \frac{3}{4}\gamma E^3 \right]^2 - \left[\frac{3}{4}\gamma\bar{x}_0^2E \right]^2 \\ & + [\lambda E\omega]^2, \end{aligned}$$

the polynomial Eq. (29) hence corresponds to

$$\varepsilon_c^2 + \varepsilon_s^2 = \varepsilon_0^2.$$

We emphasize that the purpose is not here to approximate ε , but rather to show the occurrence of hysteresis and its influence upon stability, particularly when the delay τ is taken into account.

References

- [1] L.M. Pecora, T.L. Carroll, *Phys. Rev. Lett.* 64 (1990) 821.
- [2] L.M. Pecora, T.L. Carroll, *Phys. Rev. A* 44 (1991) 2374.
- [3] M. Lakshamanan, K. Murali, *Chaos in Nonlinear Oscillators, Controlling and Synchronization*, World Scientific, Singapore, 1996.
- [4] T. Kapitaniak, *Phys. Rev. E* 50 (1994) 1642;
T. Kapitaniak, *Controlling Chaos*, Academic Press, London, 1996.
- [5] S. Boccaletti, A. Farini, F.T. Arecchi, *Phys. Rev. E* 55 (1997) 4979.
- [6] R. Fermat, J. Alvarez-Ramirez, *Phys. Lett. A* 236 (1997) 307.
- [7] N.J. Corron, D.W. Hahs, *IEEE Trans. Circ. Syst. I* 44 (1997) 373.
- [8] P. Wofo, *Phys. Lett. A* 267 (2000) 31.
- [9] K. Murali, M. Lakshamanan, *Phys. Lett. A* 241 (1998) 303.
- [10] C. Pezeschki, E.H. Dowell, *Physica D* 32 (1988) 194.
- [11] U. Parlitz, W. Lauterborn, *Phys. Lett. A* 107 (1985) 351.
- [12] A.H.-D. Cheng, C.Y. Yang, K. Hackl, M.J. Chajes, *Int. J. Nonlin. Mech.* 28 (1993) 549.
- [13] A.H. Nayfeh, D.T. Mook, *Nonlinear Oscillations*, Wiley, New York, 1979.
- [14] J.J. Stocker, *Nonlinear Vibrations in Mechanical and Electrical Systems*, 1950.
- [15] C. Hayashi, *Nonlinear Oscillations in Physical Systems*, McGraw-Hill, New York, 1964.
- [16] G. Malescio, *Phys. Rev. E* 53 (1996) 2949.
- [17] N.J. Corron, *Phys. Rev. E* 63 (2001) 055203.
- [18] P. Ashwin, J. Buescu, I. Stewart, *Phys. Lett. A* 193 (1994) 126.
- [19] B. Mensour, A. Longtin, *Phys. Lett. A* 244 (1998) 59.
- [20] H.U. Voss, *Phys. Rev. E* 61 (2000) 5115.